

Supplement of

Wintertime Extreme Warming Events in the High Arctic: Characteristics, Drivers, Trends and the Role of Atmospheric Rivers

Weiming Ma¹, Hailong Wang¹, Gang Chen², Yun Qian¹, Ian Baxter^{3,4}, Yiling Huo¹, Mark W. Seefeldt⁵

¹Atmospheric Sciences and Global Change Division, Pacific Northwest National Laboratory, Richland, WA, USA

²Department of Atmospheric and Oceanic Sciences, University of California Los Angeles, Los Angeles, CA, USA

³Department of Geography, University of California, Santa Barbara, Santa Barbara, CA, USA

⁴Earth Research Institute, University of California, Santa Barbara, Santa Barbara, CA, USA

⁵National Snow Ice and Data Center, University of Colorado Boulder, Boulder, CO, USA

Correspondence to: Weiming Ma (weiming.ma@pnnl.gov), Hailong Wang (Hailong.Wang@pnnl.gov)

Contents of this file:

Text S1

Figures S1 to S5

Introduction

Text S1 describes the method used in section 3.4 to decompose AR trends into a dynamical component and a thermodynamic component. Figure S1 shows the spatial patterns of mean warming event frequency. Figure S2 shows the climatology of surface sensible heat flux and latent heat flux during winter of 1979-2021. Figure S3 shows the temporal evolution of T2m anomalies and integrated water vapor transport (IVT) for warming events. Figure S4 shows the trends in AR frequency and its dynamical and thermodynamic component. Figure S5 shows the trends in the column-integrated water vapor (IWV) and the 850 mb wind magnitude.

Text S1:

Following Ma et al. (2020), a scaling method is applied to the IVT to decompose the total AR trends into a dynamical component, which is driven by changes in the atmospheric circulation, and a thermodynamic component, which is due to changes in the moisture field. To obtain the dynamical component, the specific humidity at each grid point (3-dimensional location) and time is scaled by a scaling factor $\frac{q_c}{q_m}$, where q_c and q_m are the winter climatological specific humidity and the seasonal mean specific humidity at a given season, respectively, at the same grid location to which this scaling factor applies. The scaled specific humidity is then combined with the wind field to calculate a scaled IVT. The scaled IVT along with the IVT threshold based on the original IVT are then used as input for the AR detection algorithm. This scaling method suppresses the interannual variability in the moisture field. Trends in the AR statistics based on the scaled IVT can thus be treated as the trends driven by changes in circulation, namely the dynamical trend. The difference between the total trend and the dynamical trend is then treated as the thermodynamic trend.

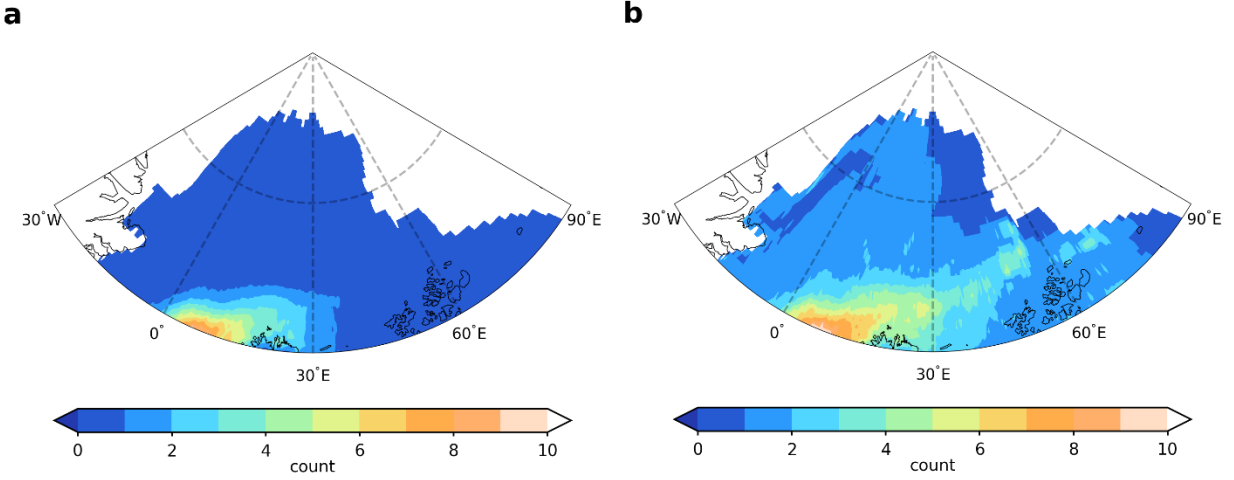


Figure S1. Spatial distribution of (a) the seasonal mean event count for all winters and for (b) only those winters with at least one extreme warming event from 1979-2021.

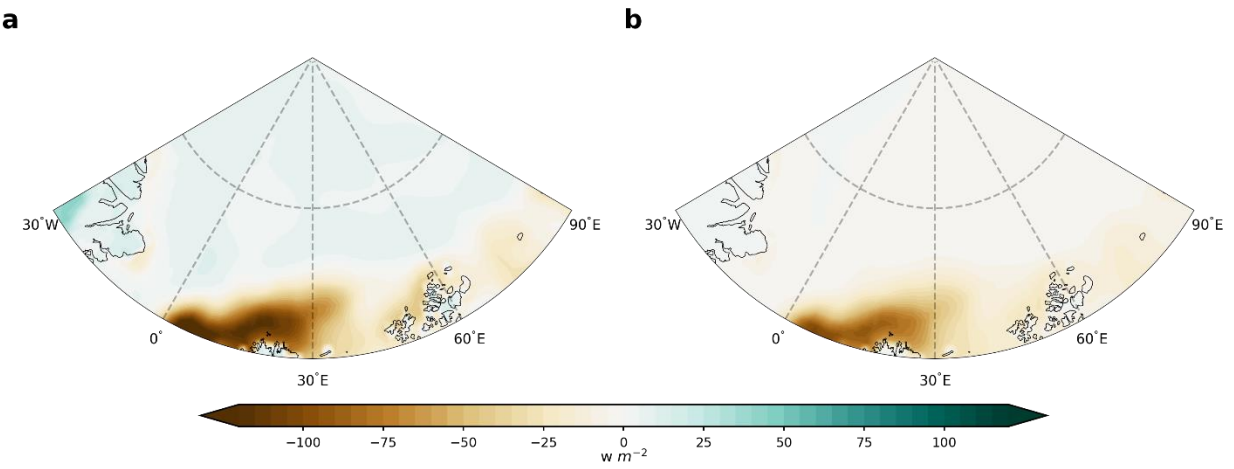


Figure S2. The climatology of (a) sensible heat flux and (b) latent heat flux during winter of 1979-2021. Positive values indicate the flux is directed downward toward the surface.

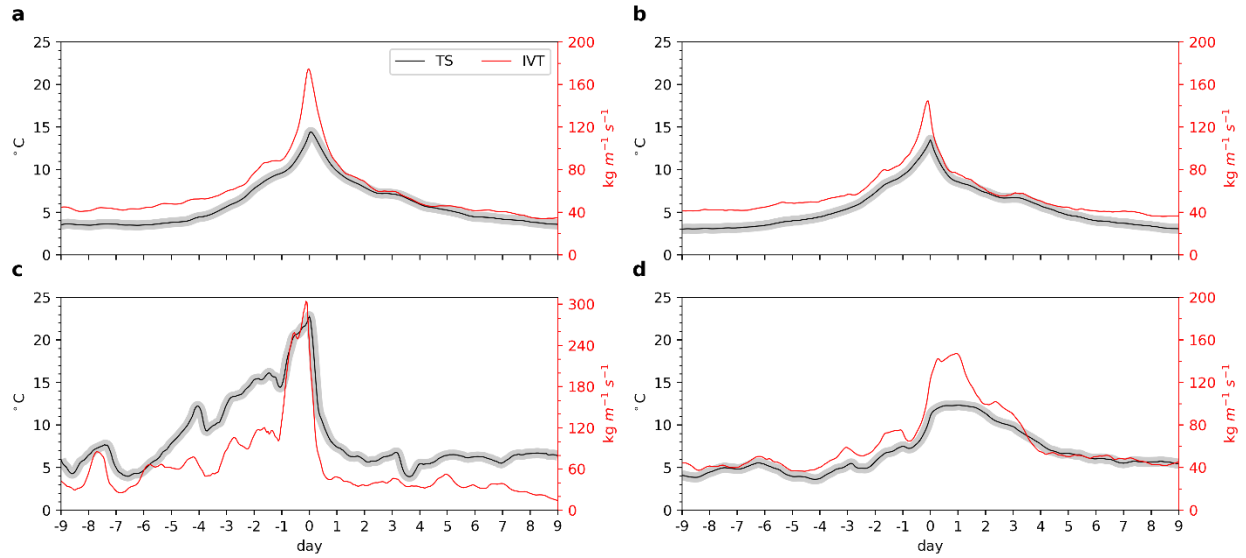


Figure S3. Temporal evolution of the T2m anomalies and IVT for (a) all the warming events, (b) short duration events equatorward of 83°N, (c) short duration events poleward of 85°N, (d) and long duration events. The shading denotes the anomalies significant at the 0.05 level based on the Student's t-test.

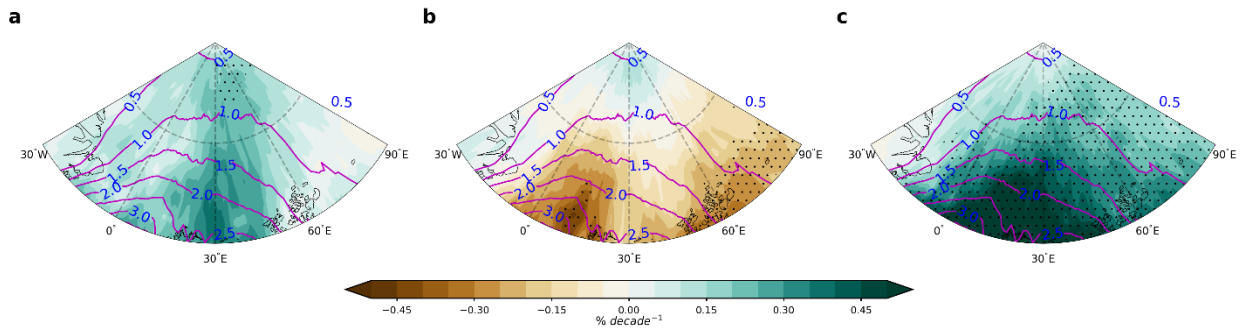


Figure S4. Spatial distribution of trends in (a) AR frequency, (b) the dynamical component and (c) the thermodynamic component. Stippled areas indicate trends significant at the 0.05 level based on the Student's t-test. The solid line contours show the climatology of the winter AR frequency (%).

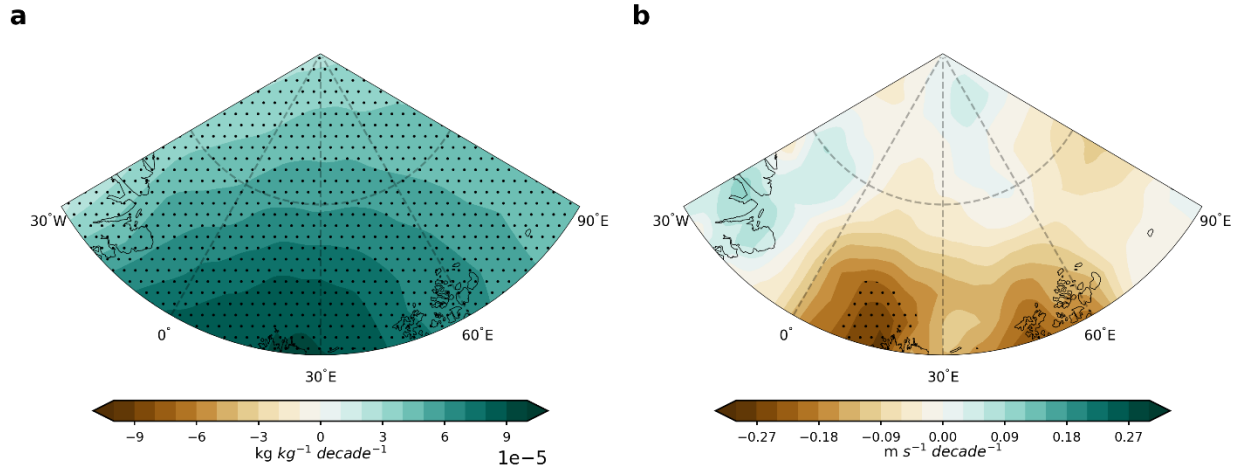


Figure S5. Spatial distribution of trends in (a) IWV and (b) 850 mb wind speed. Stippled areas indicate trends significant at the 0.05 level based on the Student's t-test.

Reference:

Ma, W., Chen, G., and Guan, B.: Poleward Shift of Atmospheric Rivers in the Southern Hemisphere in Recent Decades, *Geophys. Res. Lett.*, 47, 1–11, <https://doi.org/10.1029/2020GL089934>, 2020.